Supplementary Information

Energy Absorption and Resilience in Quasi-Static Loading of Foam-Formed Cellulose Fibre Materials

Elina Pääkkönen[1], Jukka A. Ketoja[1,*], Jouni Paltakari[2]

[1]VTT Technical Research Centre of Finland Ltd, Solutions for Natural Resources and Environment, Koivurannantie 1, FI-40400 Jyväskylä, Finland

[2] Aalto University, Department of Bioproducts and Biosystems, Aalto University, P.O. Box 11100, 00076 Aalto, Espoo, Finland; Jouni.Paltakari@aalto.fi

*Corresponding author: jukka.ketoja@vtt.fi

Work associated with inelastic fibre buckling

The compression stress causes individual fibre segments to bend. During material loading, the critical internal bending moment of a fibre may be exceeded, which can cause the segment (or fibre wall) to buckle inelastically. This can drastically decrease the ability of the segment to carry load, which leads to a re-distribution of the stress between neighbouring fibre segments.

The maximal axial load carried out by a segment of length $a_0 s(\epsilon)$ can be estimated as

$$F = \frac{kE_{mod}I}{[a_0 s(\epsilon)]^2} \quad \text{(S1)}$$

where a_0 is the mean segment length of the network, E_{mod} is the elastic modulus, I is the area moment of inertia, and k is a coefficient that depends on the boundary conditions at the segment ends (affected by bonding properties). After the elastic deformation, the segment has a curved shape with strong local strain and stress profiles as shown in Fig. S1a. These internal stresses can further trigger an inelastic buckling in the segment, leading to a plastic hinge as shown in Fig. S1b. The bending momentum at the hinge can be estimated as

$$M = F\ sin(\theta) a_0 s. \quad \text{(S2)}$$

The energy associated with the inelastic buckling becomes

$$W = \int M d\theta = -2F a_0 s \Delta cos(\theta) \sim k E_{mod} I/(a_0 s) \sim 1/s, \quad \text{(S3)}$$

which agrees with the interpretation of the integral of Eq. (7) as the total internal deformation energy of the fibre network.

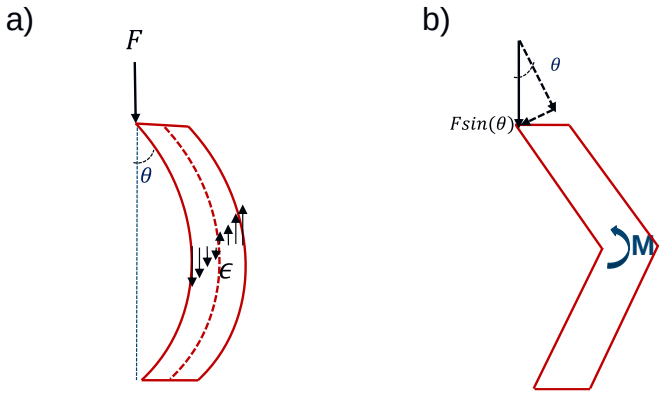

Fig. S1 *a) Strain profile (leading to a similar stress profile) in a bended fibre segment with an axial load F. Here, the deformation of a segment is considered using its initial non-loaded state as a reference. The dried-in stresses generally cause a fibre to have a curly shape, but for simplicity, such initial stresses without external loading are omitted. b) When the critical internal bending momentum of the fibre is exceeded, the inelastic buckling is driven by the bending momentum M at the formed plastic hinge.*

Surfactant residues in foam-formed samples

To foster a better understanding of the safety of the material, surfactant residue from the selected samples were spectrophotometrically analysed as described for SDS in relevant literature (Viitala et al. 2020; Ketola et al. 2022). One or two replicates were made for one trial point. The determination of PVA residue in the samples was done with the following procedure. The dry sample was disintegrated in ca. 300 mL of deionised water. Then, the fibre suspension was heated to 95–96 °C for 30 min. The heated fibre suspension was filtered through filter paper (Whatman 40) and washed with 100 ml of hot deionised water. Next, it was washed two times with 50 ml 1:1 HCl solution. Finally, it was washed with 200 ml of deionised water. The filtrate was diluted to a final volume of 1000 mL. About 100 mL of filtrate was centrifuged at 2200 rpm for 10 min. The PVA content of the filtrate was measured with a spectrophotometer (Hach Lange DR3900 VIS, United States). Calibration curves were created with known concentrations of PVA.

Table S1 shows that when the mixture of SDS and Tween was used, the surfactant residues were much lower (1.5 mg/g) compared to the use of just SDS. The obtained level with SDS, 6.3–11.1 mg/g, is more comparable with the theoretical estimate 8.6 mg/g obtained by assuming 10% solids content before drying. Regarding the higher strength obtained with PVA, it is an interesting point that the PVA residue appeared to be higher in CTMP samples (14.5–15.4 mg/g) than in BSKP samples (11.9 mg/g). However, more tests should be done to verify this dependence on the pulp type. Nevertheless, the theoretical PVA 6-88 residue (assuming 10% solids content before drying) is much higher, 25.7 mg/g. Overall, these results indicate that from a material safety point of view, the use of surfactant mixtures instead of one surfactant should be preferred.

Table S1. The analysed surfactant residues from a few selected trial points.

Sample ID	Fibre type	Surfactant type	Surfactant dosage (g/l)	SDS residues (mg/g dry fibre)	PVA 6-88 (mg/g dry fibre)
1_1	BSKP	SDS	1.0	6.96	
1_2	BSKP	SDS	1.0	11.1	
2_1	BSKP	SDS	1.0	6.25	
2_2	BSKP	SDS	1.0	6.57	
3_1	BSKP	SDS	1.0	10.1	
3_2	BSKP	SDS	1.0	8.78	
4_1	CTMP	SDS	1.0	6.35	
4_2	CTMP	SDS	1.0	7.00	
5_1	BSKP	SDS + Tween 20	0.5+0.5	1.51	
6_1	BSKP	PVA 6-88	3.0		11.9
7_1	CTMP	PVA 6-88	3.0		14.5
7_2	CTMP	PVA 6-88	3.0		15.4

Effect of surfactant type on compression strength

The effect of surfactant type on compression strength and recovery was evaluated with both unrefined BSKP and CTMP (CSF 650), and a part of the results gained with SDS, Tween and PVA were discussed in our earlier work (Ketoja et al. 2019). In this paper, some additional trial points were obtained with Berol, APG, and a mixture of SDS and Tween. With BSKP, the highest compression strength was attained with PVA (**Fig. S2**). On the other hand, nonionic Tween and anionic SDS led to similar results. The number of data points obtained with Berol, APG and the mixture of SDS and Tween were rather limited, but they seem to be more in line with data obtained with SDS and Tween than with PVA. These results are similar to those of Pöhler et al. (2020), who stated that a PVA mixture led to a stronger, but more uneven material than the one obtained with SDS.

Similar results are illustrated in **Fig. S3** for CTMP. Using PVA, a bit higher compression strength was achieved than with the other foaming agents, but the difference was smaller than with BSKP. Based on the results, we can conclude that PVA leads to a bit higher strength than the other surfactants, but otherwise, the effect of surfactant on compression stress is negligible for the type of pulps studied here.

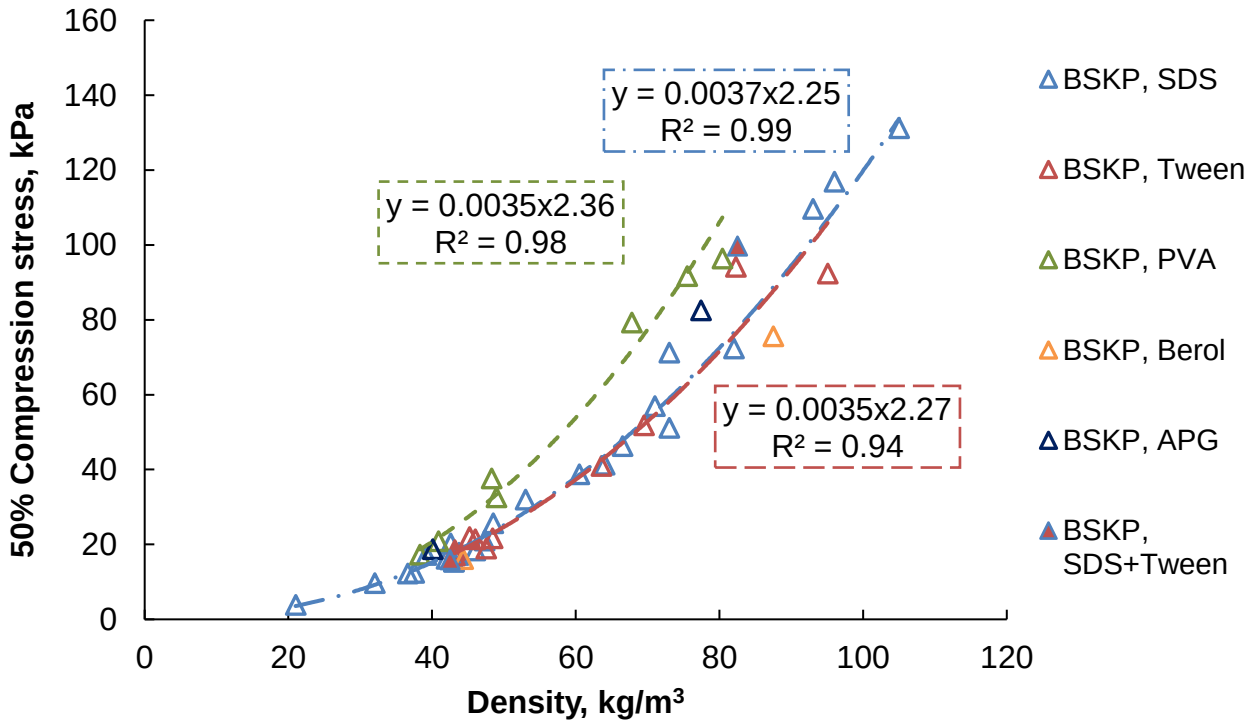

Fig. S2 *The effect of surfactant type on compression strength with BSKP at 50% compression.*

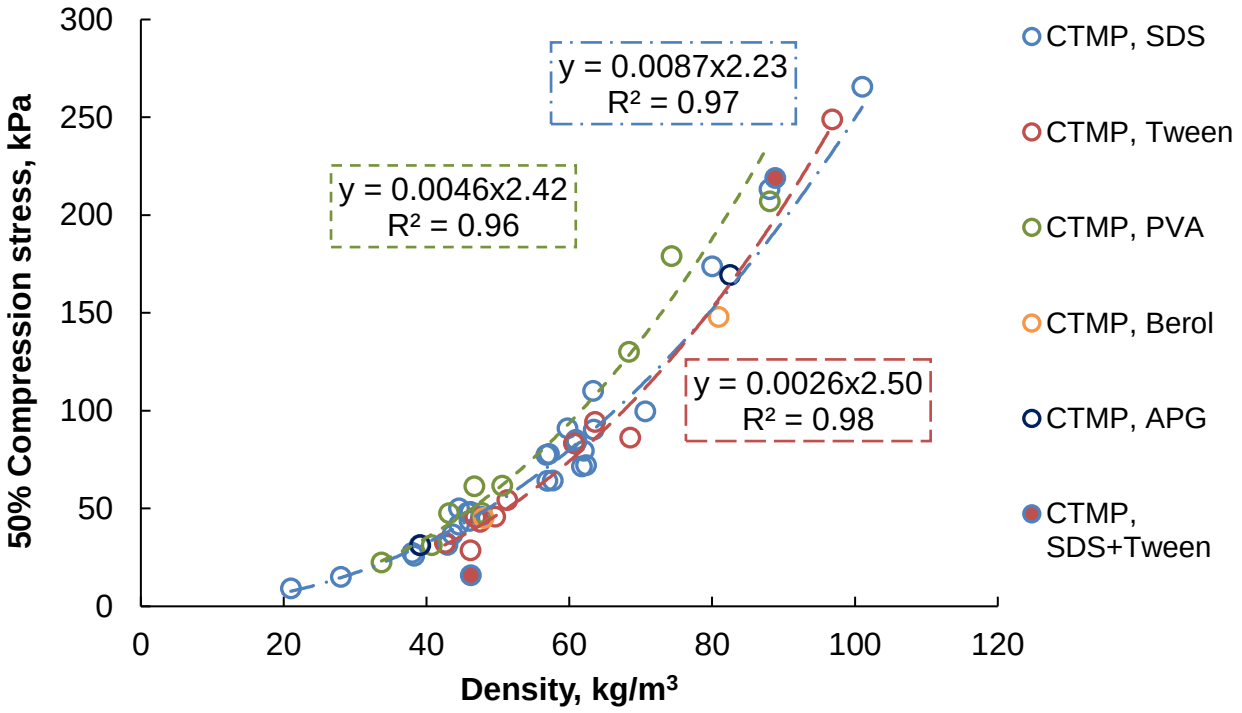

Fig. S3 *The effect of surfactant type on compression strength with CTMP at 50% compression.*

The effect of strength additives

A few different additives were tested to enhance the strength properties. The selected additives were cationic starch (starch, Raisamyl 50021, Chemigate), cationic polyacrylamide (C-PAM, FennoBond 46, Kemira) and microfibrillated cellulose (MFC, code E505SWM4). MFC was refined four times by an ultrafine friction grinder (MKZA10-15J, VTT).

Fig. S4 and **Fig. S5** present the compression stress at a target density of 40 kg/m^3. Here we took advantage of the earlier power-law formulas of Figure 4 to interpolate the nearest measured data point to the target density. When comparing the results at the 40 kg/m^3 density level, refining clearly improved the compression strength for the BSKP sheets for all the tested surfactant types. The highest strength was achieved with the refining level of SR36 using PVA as the foaming agent. Also statistically, the effect of the pulp refining level on compression strength was seen as significant, p(2-tailed) = 0.356. The effect of additives on the strength was studied using PVA as a foaming agent. The addition of starch improved the compression strength slightly, but C-PAM did not affect the compression strength. The use of CMF also had a positive effect on the compression strength when

added to the unrefined (SR13) pulp, but the strengthening effect was not seen with a higher refining level at which the pulp could already include more fines.

The compression strength of CTMP sheets was not improved by using a lower freeness level CTMP (**Fig. S5**). The reason may be the different types of fines of the CTMP. The addition of starch, CMF or C-PAM had only a minor effect on the compression strength. However, the simultaneous addition of starch and CMF led to the highest compression strength and recovery. Paunonen *et al.* (2018) achieved even higher recovery for CTMP sheets, especially with latex. In their study, the latex probably made inter-fibre joints more elastic and therefore the recovery improved.

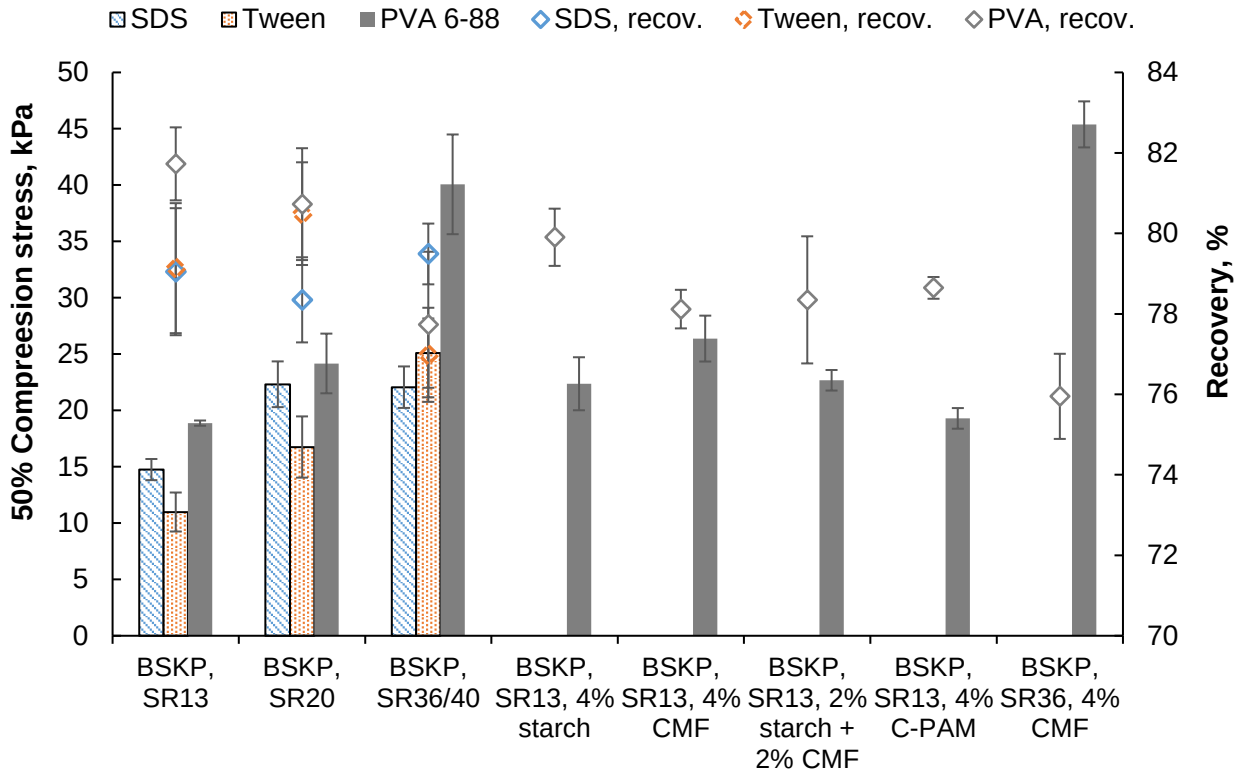

Fig. S4 *The effect of refining level and additives on compression strength at 50% strain (columns) and recovery (diamonds) for the BSKP samples. Compression stress results have been normalised to a density of 40 kg/m^3 (see text). Error bars represent the standard deviation among the data set.*

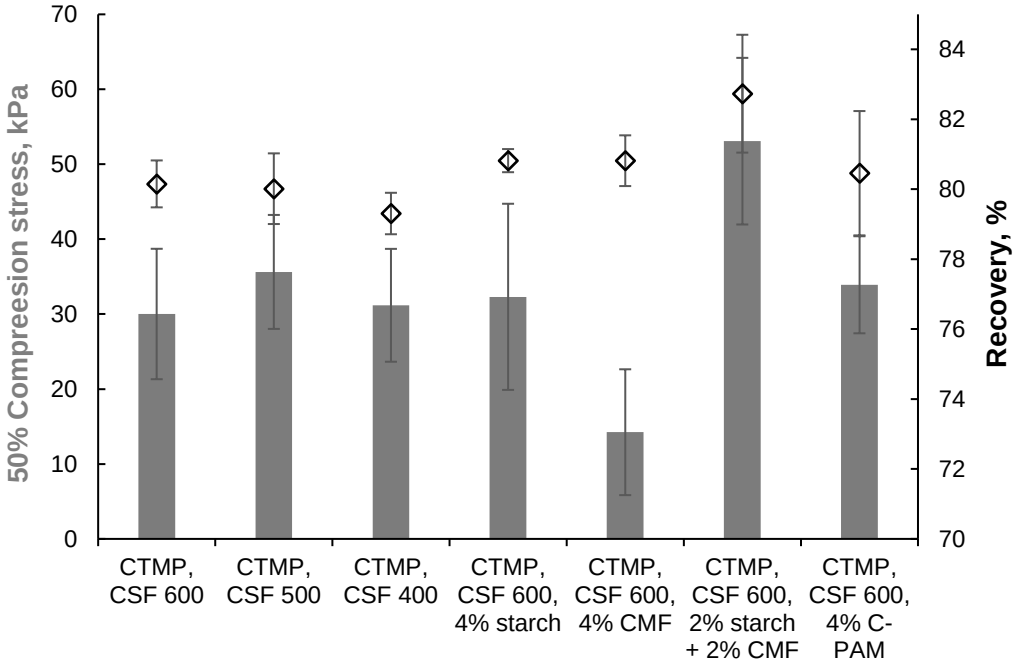

Fig. S5 *The effect of refining level and additives on the compression strength at 50% strain and on the recovery for the CTMP samples. Compression stress results (columns) have been normalised to a density of 40 kg/m^3 (see text). Recovery of the material is presented by diamonds. PVA 6-88 was used as a foaming agent for all trial points. Error bars represent the standard deviation among the data set.*

Cushion factor

Fig. S6 shows how the obtained cushion factor is affected by the shape of the stress-strain curve. We reflect the cushion factor against the mean square deviation of the measured stress-strain curve from the theoretical curve obtained for an ideal random fibre network.

For samples that have the smallest deviations from the theory prediction, the cushion factor is also close to the predicted value of 4.61. To get values away from this level requires that the whole stress-strain curve is altered, which is seen as a higher deviation value.

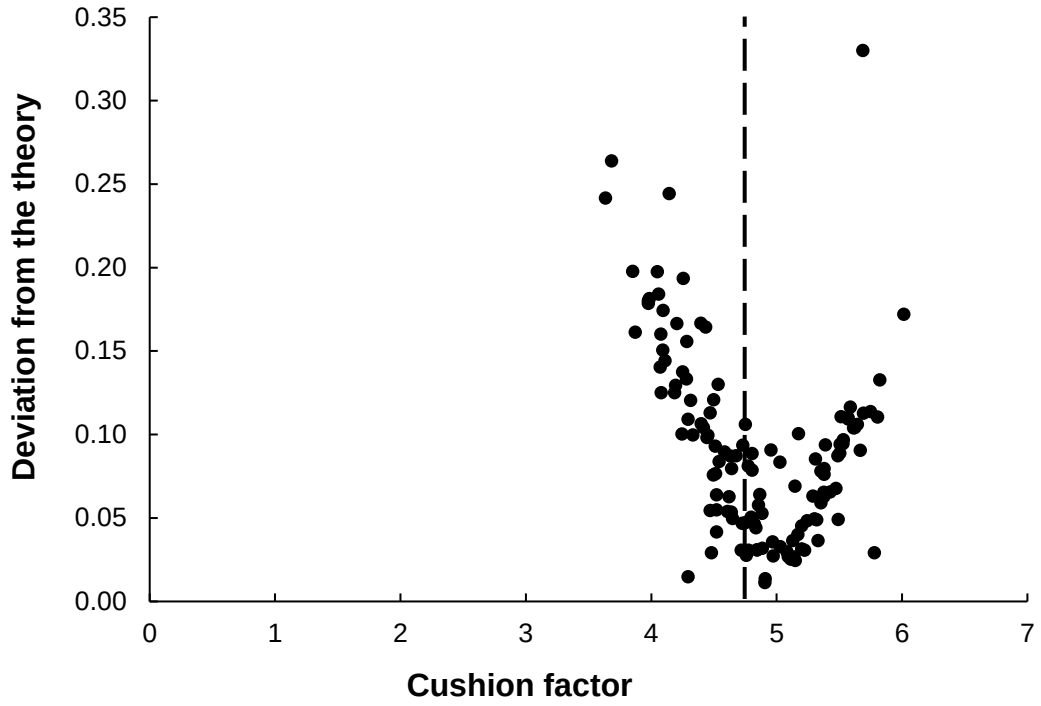

Fig. S6 *Measured cushion factor vs. mean square deviation of the corresponding stress-strain curve from the theoretical curve of Eq. (5). The dashed line indicates the theoretical value of 4.61 for an ideal random fibre network at* $\epsilon = 0.5$.

Recovery of foam-formed samples

Recovery from compression of all of the studied trial points is compared to EPS in Fig. S7.

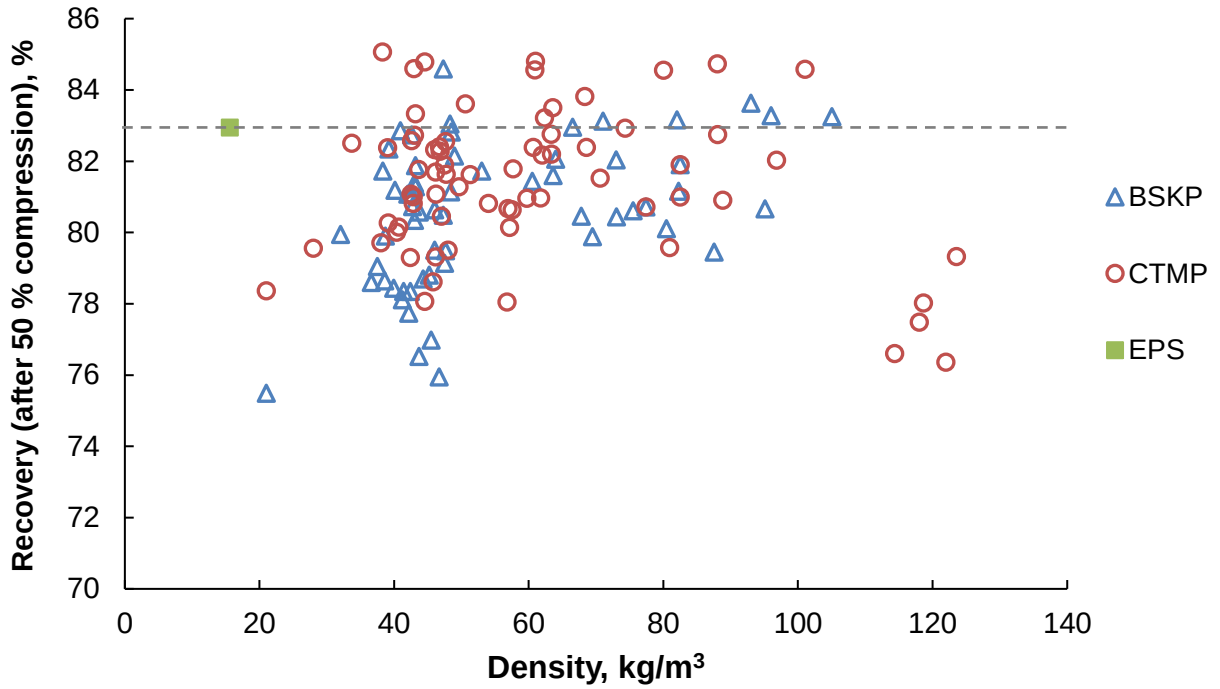

Fig. S7 *Recovery from 50% compression for all produced samples compared to that of EPS.*

Fig. S8 presents the effect of surfactant type on recovery with CTMP samples. The highest recoveries were seen with the SDS, and then with PVA, but quite a high variation was seen in the samples.

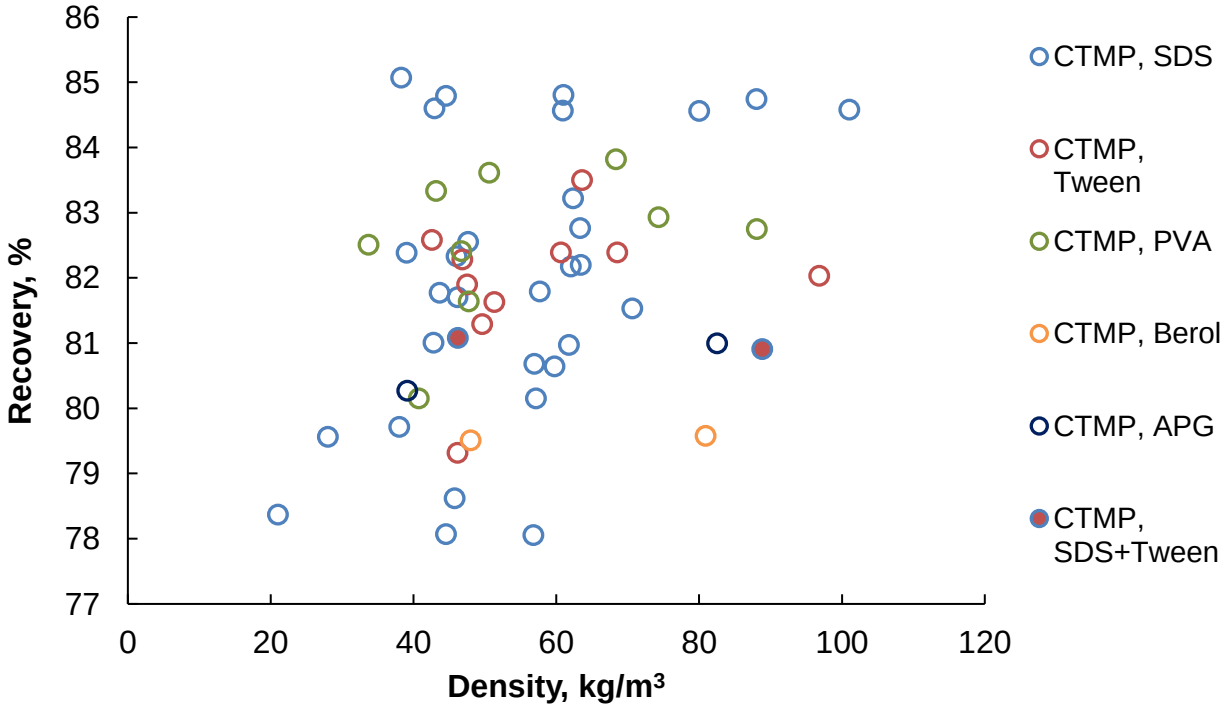

Fig. S8 *The effect of surfactant type on recovery with CTMP at 50% compression.*

References

Ketoja JA, Paunonen S, Jetsu P, Pääkkönen E (2019) Compression strength mechanisms of low-density fibrous materials. Materials 12:384. https://doi.org/10.3390/ma12030384

Ketola AE, Song W, Lappalainen T, Salminen K, Viitala J, Turpeinen T, Miettinen A, Lee K-Y, Ketoja JA (2022) Changing the structural and mechanical anisotropy of foam-formed cellulose materials by affecting bubble−fiber interaction with surfactant. ACS Appl Polym Matter 4:7685–7698. https://doi.org/10.1021/acsapm.2c01248

Paunonen S, Timofeev O, Torvinen K, Turpeinen T, Ketoja JA (2018) Improving compression recovery of foam-formed fiber materials. Bioresources 13:4058–4074

Pöhler T, Ketoja JA, Lappalainen T, Luukkainen V-M, Nurminen I, Lahtinen P, Torvinen K (2020) On the strength improvement of lightweight fibre networks by polymers, fibrils and fines. Cellulose 27:6961–6976. https://doi.org/10.1007/s10570-020-03263-x

Viitala J, Lappalainen T, Järvinen M (2020) Sodium dodecyl sulphate (SDS) residue analysis of foam-formed cellulose-based products. Nord Pulp Paper Res J 35:261–271. https://doi.org/https://doi.org/10.1515/npprj-2019-0058